




Finite Element Analysis of Neonatal Skull Stress During 3D Printed Nasoalveolar Molding Therapy for Cleft Lip and Palate



Bahoz H. Majeed^{1,*} , Mustafa M. Alsultan²  and Zhala D. Omar³ 

¹Department of Orthodontics, College of Dentistry, University of Duhok, Duhok, Iraq

²Department of Orthodontics, College of Dentistry, Al Hadbaa University College, Mosul, Iraq

³Department of Prosthodontics, College of Dentistry, Hawler Medical University, Erbil, Iraq

Abstract:

Introduction: Orofacial clefts, including Cleft Lip and Palate (CLP), are common congenital disabilities that often require non-surgical treatments like Nasoalveolar Molding (NAM) therapy. This study aimed to assess stress distribution and potential deformation in both the viscerocranium and neurocranium of a 17-day-old neonate skull with unilateral cleft lip and palate using Finite Element Analysis (FEA) under different applied forces.

Methods: This research was conducted in Erbil province from August 2024 to November 2024. MIMICS, 3-Matic Medical, and ANSYS programs were used to determine the effects of Nasoalveolar Molding (NAM) therapy on cranial and facial structures. This study included neonates who were 17 days old, diagnosed with nonsyndromic unilateral cleft lip and palate, and had a normal head circumference.

Results: The results showed varying von Mises stress distributions, with maximum stress values of 77,053 Pa at 0.75 N, which exceeded the deformation threshold of 30,000 Pa, indicating potential viscerocranial deformation. Lower forces (0.65 N and 0.70 N) remained below this threshold.

Discussion: The study confirmed that forces exceeding 30,000 Pa during Nasoalveolar Molding (NAM) therapy led to potential deformation in the neonatal viscerocranium. Finite element analysis showed that a force of 0.75 N generated stress above this threshold.

Conclusion: The applied force during Nasoalveolar Molding (NAM) therapy plays a crucial role in preventing craniofacial deformation in neonates with unilateral cleft lip and palate. Therefore, managing force levels in Nasoalveolar Molding (NAM) therapy is essential to avoid potential long-term deformation.

Keywords: Finite element analysis (FEA), Nasoalveolar molding (NAM), Unilateral cleft lip and palate, Von mises stress, Congenital disabilities, Cranial and facial structures.

© 2025 The Author(s). Published by Bentham Open.

This is an open access article distributed under the terms of the Creative Commons Attribution 4.0 International Public License (CC-BY 4.0), a copy of which is available at: <https://creativecommons.org/licenses/by/4.0/legalcode>. This license permits unrestricted use, distribution, and reproduction in any medium, provided the original author and source are credited.

*Address correspondence to this author at the Department of Orthodontics, College of Dentistry, University of Duhok, Duhok, Iraq; E-mail: bahozhmajeed@gmail.com

Cite as: Majeed B, Alsultan M, Omar Z. Finite Element Analysis of Neonatal Skull Stress During 3D Printed Nasoalveolar Molding Therapy for Cleft Lip and Palate. Open Dent J, 2025; 19: e18742106386858. <http://dx.doi.org/10.2174/0118742106386858250617103542>



Received: January 26, 2025

Revised: April 09, 2025

Accepted: May 09, 2025

Published: June 23, 2025



Send Orders for Reprints to
reprints@benthamscience.net

1. INTRODUCTION

Congenital disabilities, or congenital anomalies, include structural, metabolic, psychological, and functional abnormalities; one of the most common is orofacial cleft, resulting from improper tissue fusion early in the developmental stage [1]. Orofacial clefts (OFCs) are defined as congenital malformations of the upper lip and/or palate caused by the incomplete fusion of facial structures during early embryonic development [2]. Orofacial Clefts (OFCs) include Cleft Lip (CL), Cleft Palate (CP), and Cleft Lip and Palate (CLP), arising from abnormal facial development and failed fusion of palatal and nasal processes during gestation [3]. The prevalence of non-syndromic clefts is reported to be around 70%, while syndromic clefts are less common but occur within broader disorder patterns [4, 5]. The prevalence of orofacial clefts is about 1 in 700 live births globally, varying by region; in the U.S., it's estimated at 1 in 1000, with higher rates among Asian and Native American babies [6]. In South Korea, a study reported prevalence rates of Cleft Palate (CP), Cleft Lip (CL), and Cleft Lip and Palate (CLP) as 5.57, 2.77, and 2.75 per 10,000 births, respectively [7]. Research on the epidemiology of facial clefts in Arab countries indicates a higher incidence of these conditions in Egypt, Saudi Arabia, and Iraq [3, 8, 9]. Orofacial clefts can result in complications such as feeding difficulties, speech impairments, and social integration challenges, often requiring surgical interventions and specialized therapies to enhance function and aesthetics [10].

Finite Element Analysis (FEA) is a numerical technique that breaks down complex structures into smaller elements to predict force distribution and mechanical behavior, making it invaluable for studying craniofacial and dental deformations [11]. Within the last decade, Finite Element Analysis (FEA) has emerged as a reasonably consistent and reproducible tool for investigating patterns of stress distribution and has been applied to research in orthodontics, orthognathic surgery, and head and facial trauma [12]. In contrast, a wide range of finite element analysis applications have emerged in the field of dentistry [13]. These applications are used to determine various loads during dental implant procedures, design optimal dental crowns and bridges, and predict stress values in Temporomandibular Joint (TMJ) treatments [14-17]. The majority of orthodontic studies applying FEA are limited to the areas of skull biomechanics, tooth movement, and mechanical loads, allowing further analysis of deformation, strain, and stress, as well as craniofacial modeling anatomy to aid in the understanding of bone remodeling [18, 19]. Finite element modeling is an appropriate method to analyze and simulate force application points that can maximize well-controlled expansion in the UCLP [20]. Many studies have aimed to determine the basic parameters for Nasoalveolar Molding (NAM) therapy in children; however, their target age populations were often older than the age at which neonatal clefts are typically treated [21-23]. Nasoalveolar Molding (NAM) is a presurgical therapy using an intraoral plate with nasal stents to align alveolar segments and nasal cartilages which improve surgical outcomes and reduce deformities [24]. However, the force applied during Nasoalveolar Molding (NAM) therapy is not standardized and varies depen-

ding on the shape and size of the cleft. Previous studies have used different forces, starting as low as 0.65 N [25].

Thus, this study aimed to determine the stress distribution and possible deformation in the neurocranial and viscerocranial regions of a 17-day-old skull of an infant with unilateral cleft lip and palate under different stress applications. Using Finite Element Analysis (FEA), the study simulated and assessed the effects of Nasoalveolar Molding (NAM) therapy on cranial and facial structures.

2. MATERIALS AND METHODS

2.1. Study Design, Ethics, and Criteria

This prospective research was conducted in the Kurdistan region of Iraq, specifically in Erbil province, from August 2024 to November 2024. The study adhered to the ethical guidelines outlined in the Declaration of Helsinki. Both the study protocol and the informed consent form were approved by the local ethics committee at the University of Duhok, College of Dentistry -Iraq, under this number (08012025-1-35). Additionally, approval was obtained to contact families for potential future research participation.

The study included a 17-day-old neonate diagnosed with nonsyndromic unilateral cleft lip and palate and had a normal head circumference. The measurement of the infant's head circumference was performed using a non-elastic tape, which was placed around the largest area of the head, starting from the top of the eyebrows and extending to the back of the head. For further analysis, a complete skull CT (Computed tomography) scan in DICOM (Digital Imaging and Communication in Medicine) format was required and was sourced from Shar Hospital. This dataset included the scan of the following bones: left zygomatic, mandible, left temporal, left palatine, left nasal, left maxilla, left lacrimal, inferior conchae, left parietal, right parietal, ethmoid, vomer, sphenoid, right zygomatic, frontal, right temporal, right palatine, right nasal, right maxilla, and right lacrimal.

2.2. 3D Model and Mesh Preparation for FEA

A CT scan of the skull was obtained from Shar Hospital on June 27, 2024, using a Sensation 16 CT scanner (Siemens Healthineers, Germany) with a resolution of 512 x 512 pixels. The scan had a pixel size of 0.300781 mm, and the dataset consisted of 65 slices with a slice thickness of 2 mm. The images were acquired using the H30s reconstruction algorithm, and the software version used was Syngo CT 2014A. The CT scan dataset was then imported into dedicated image analysis software, MIMICS® (Mimics Medical 21.0.0.406, Materialise NV, Leuven, Belgium), for further processing.

In MIMICS®, a predefined CT bone threshold was selected to isolate the hard tissues of the cranium and maxilla, resulting in the creation of an optimal-quality 3D model. To refine the data, the Region Growing algorithm was employed to eliminate any floating pixels, and local threshold adjustments were made to specific regions within the segmentation mask. The mask was then edited by splitting it to target specific regions for further refinement selectively. A smoothing mask filter was applied to enhance the quality of the borders. The maxillary and alveolar bones

were modeled with a reduced thickness compared to the rest of the skull. In contrast, the other cranial regions were assigned greater thickness. Additionally, a finer geometric detail was applied to the maxillofacial region to more accurately capture the bone structure for the analysis.

The edited 3D model was imported into 3-MATIC® (3-Matic Medical 13.0, Materialise NV, Leuven, Belgium) for further refinement and preparation for analysis. Rectangular clipping was initially applied to isolate the working region of the skull. Following this, the brush and the lasso area mark tools were applied to find and locate small pores and roughnesses of the model, which were later filled using the fill hole option. To depict the triangle edges, the smooth shaded option was selected, and the diagnostic fix wizard was used to rectify any orientation problems with the triangles' assets. Following the volume mesh, a default cut and standard section were employed. Using cross-sectioning in this manner enabled model quality control and verification of the internal bone structures meshing. Following the completion of the above steps, essential components such as surface definitions and boundary conditions were defined. Additionally, the skull anatomical structure was further sectioned into different volumetric regions with appropriate mesh to enhance computing efficiency while modeling the interaction of the teeth and dental germs. Ultimately, both the residuals uniform mesh and volume mesh were generated to prepare the model for the finite element analysis.

2.3. Development of Finite Element Model

The ANSYS ICEM CFD (Integrated Computer Engineering and Manufacturing - Computational Fluid Dynamics) (ANSYS 2020 R1, ANSYS Inc., Pennsylvania, USA) software, which specializes in CFD modeling, was employed for the meshing of the skull model. However, in the present work, some resolution change was needed in different regions of the model. The octree meshing method was used for the model that was developed with 2nd-order SOLID185 elements, generating approximately a range of 500,000 to 650,000 nodes. A geometric deviation cutoff of 0.01 mm was separated for this study and was sufficient to provide a quality model for performing finite element analysis (FEA).

Herein, 3D meshes corresponding with the given model were imported back into the MIMICS® (Mimics Medical 21.0.0.406; Materialise NV; Leuven, Belgium) package, where material properties were assigned to each mesh element. These were based on the Gray Values (GV) corresponding to the Hounsfield units (HU) of the scanned tissues, as determined by CT scan results. This enables the representation of various materials for the models, like bone and soft tissue, by associating their density values with the corresponding hyper mesh regions.

The boundary conditions were formulated in ANSYS APDL (ANSYS Parametric Design Language 16.0, ANSYS, Inc.; Pennsylvania, USA) via custom scripting for the simulation. Ultimately, after setting boundary conditions, the model was solved and the binary solution file was post-processed with ANSYS CFD-Post (ANSYS CFD-Post, ANSYS, Inc.; Pennsylvania, USA) for analysis and visualization,

which enables thorough post-processing and analysis of simulation results. Fig. (1) shows the process of FEA meshing and neonatal skull model creation (CT image process, mesh development, properties assigned, boundary conditions).

2.4. Material Properties, Boundary Conditions, and Mechanical Forces

The neonatal skull bone was modeled as an isotropic, linearly elastic material, with mechanical properties estimated from Gray Values (GV), which represent bone density (method source:0). The GV range was split into 50 sections, and the elastic modulus was determined through the relationship between bone density at the local level and GV-based (McPherson & Kriewall 1980 ref data). Mimics projected these material properties on the model to achieve an accurate representation of the bone structure in the finite element analysis.

Linear interpolation of the known values for E-modulus in a newborn (0 days) and 4-week-old infant (28 days) skull was performed using the data from a previous study [26]. The linear interpolation formula was used to estimate the range for a 17-day-old infant skull (Eq. 1). E-modulus for newborns was found to be lowest at 1337 MPa and highest at 3367 MPa, while E-modulus for 4-week-old infants was minimum at 1737 MPa and maximum was 3367 (Eqs. 2, and 3) according to the linear interpolation formula [27]:

$$y = y_1 + \frac{(x - x_1) \cdot (y_2 - y_1)}{x_2 - x_1} \quad (1)$$

The following calculations were performed, where X is the target age (17 days). Regarding the lowest E-modulus:

$$E_{\min target} = 1337 + \frac{(17 - 0) \cdot (1737 - 1337)}{28 - 0} \approx 1579.86 \text{ MPa} \quad (2)$$

For the maximum E-modulus:

$$E_{\max target} = 3367 + \frac{(17 - 0) \cdot (3767 - 3367)}{28 - 0} \approx 3609.86 \text{ MPa} \quad (3)$$

Accordingly, the predicted E-modulus range for the skull of a 17-day-old newborn was roughly 1,580 MPa to 3,610 MPa.

The aim was to explore stress distribution, cleft width influence, von Mises stress, and deformations in a 17-day-old neonatal skull subjected to forces of weight 0.65 N, 0.70 N, and 0.75 N, respectively. These forces, among others, were applied in the two localization points of the virtual model to study the influence of stress on skull behavior under these mechanical conditions. The disappearance of deformation from the skull was identified using a critical threshold of stress 30,000 Pa as probably happening over a period that particularly applies to positional plagiocephaly. The threshold was selected for its direct applicability to the various degrees of deformation observed in positional skull shapes and acts as a baseline of sorts for assessing changes in shape due to long-lived effects from similar mechanical loading.

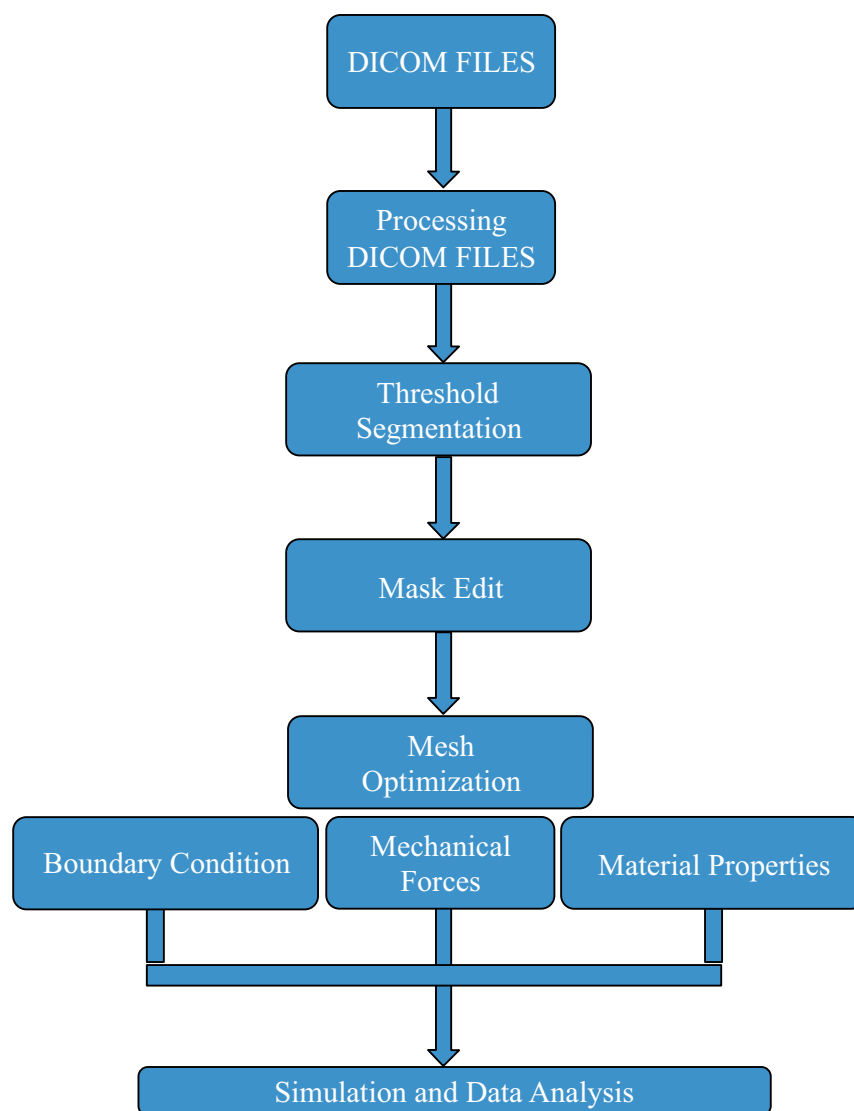


Fig. (1). 3D model and mesh preparation for FEA.

2.5. Data Analysis

The results of the finite element analysis were evaluated using ANSYS CFDPost (ANSYS, Inc.; Pennsylvania, USA) to examine stress distribution and deformation patterns. Stress values corresponding to forces of 0.65 N, 0.70 N, and 0.75 N were compared, with a focus on von Mises stress, and assessed against a 30,000 Pa threshold to identify potential deformation risks. Descriptive statistics were then applied to summarize the data and analyze the effects of different force levels.

3. RESULTS

FEA results of the neonatal skull bones force distribution (Fig. 2) were further used to illustrate the stress uniformly across the skull in finite element analysis. In Fig. (2), von Mises stress distribution was determined to study the effects of three different forces (0.65 N, 0.70 N, and 0.75 N) on skull regions. The study revealed substantial stress hot-

spots at the maxilla, vomer, ethmoid, zygomaticus, temporalis, lacrimalis, and sphenoid bone, expressing that each force had a unique effect on skull structure. At a force of 0.75 N, the simulation results showed that the applied force traveled more extensively across the palate, from the point of application to the opposite side, compared to the lower forces of 0.65 N and 0.70 N in the 17-day-old neonatal skull with unilateral cleft lip and palate.

The maximum stress values observed were 57,717 Pa for 0.65 N, 63,200 Pa for 0.70 N, and 77,053 Pa for 0.75 N, as shown in Fig. (3) and Table 1. The arithmetic mean stress values for each force were calculated as 26,207 Pa for 0.65 N and 28,346 Pa for 0.70 N, both of which were below the threshold value of 30,000 Pa derived from a plagiocephaly case. However, for 0.75 N, the mean stress exceeded the threshold, indicating that the applied force at this level could potentially lead to viscerocranial deformation. This comparison was used to validate the simulation results and identify stress patterns of concern.

Table 1. Maximum von Mises stress values [Pa] for the finite element model of a 17-day-old neonate skull under different applied forces. The peak stress was identified as the value at the 99.9th percentile.

Model	Force 1	Force 2	Force 3
Global Peak von Mises stress [Pa]	57717	63200	77053

4. DISCUSSION

This study aimed to calculate, evaluate, and predict the stress distribution and potential deformation in a 17-day-old neonate skull with unilateral cleft lip and palate under varying mechanical forces during Nasoalveolar Molding (NAM) therapy. It focused on force levels that could lead to deformation, hypothesizing that stresses exceeding 30,000

Pa in the viscerocranium and neurocranium during NAM therapy may cause structural changes.

Modeling biological systems presents significant challenges due to their complex geometry, material heterogeneity, and nonlinear behavior [28]. These complexities are particularly evident in the context of bone metabolism and healing, where hormones play a crucial regulatory role, especially in conditions like cleft lip and palate [29]. Key hormones, including estrogen, testosterone, parathyroid hormone, insulin, oxytocin, cortisol, angiotensin, adiponectin, and erythropoietin, significantly influence bone formation and remodeling [29, 30]. These hormonal effects are critical for bone recovery in the craniofacial region, which is especially relevant during surgical interventions or orthodontic procedures [29]. However, the scarcity of infant samples further complicates the development of accurate Finite Element (FE) models, with only a limited number of studies addressing this issue to date [31-38].

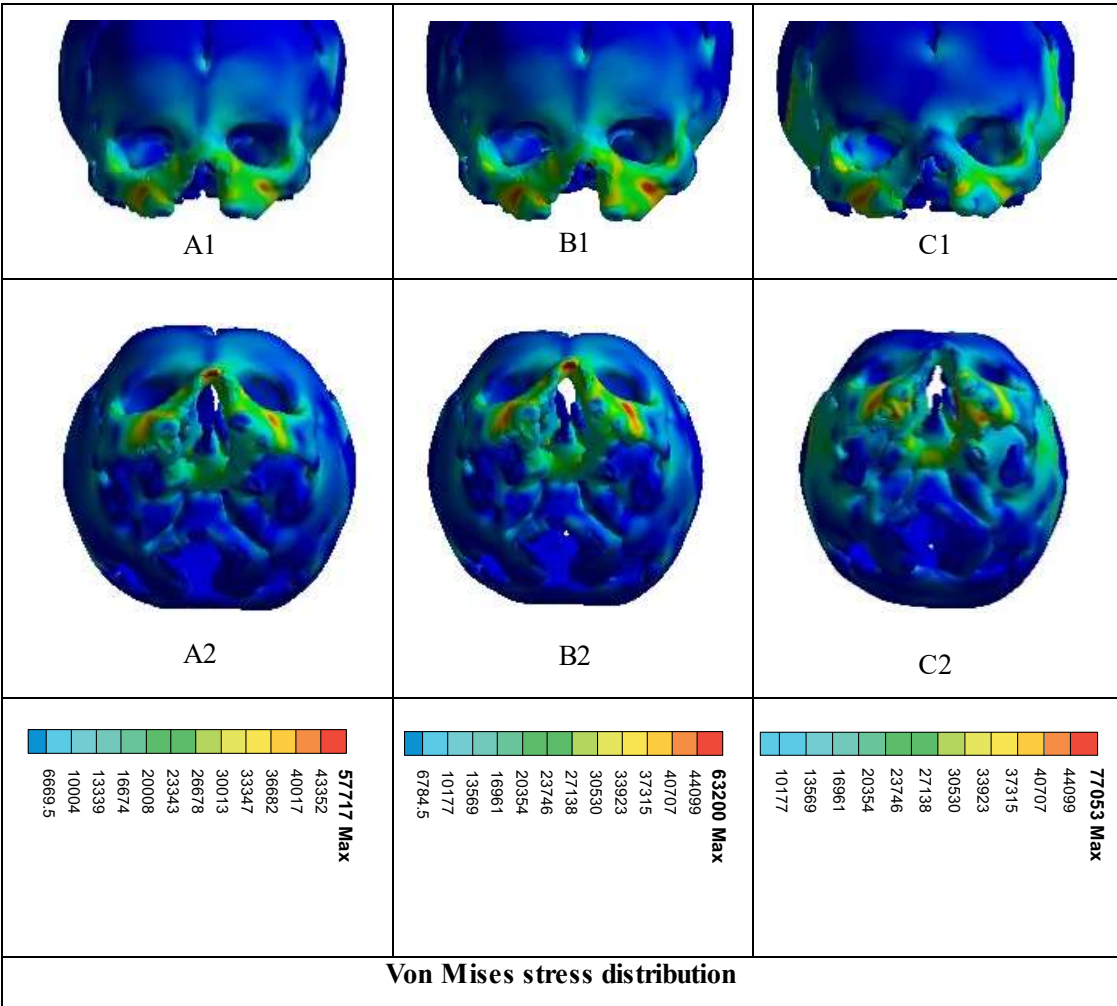


Fig. (2). Von Mises stress distribution in the simulated skull of a 17-day-old patient. The lower row displays the inferior (base) view of the skull, while the upper row shows the anterior view. Panels A1 and A2 represent the stress distribution for a force of 0.65 N, B1 and B2 for 0.70 N, and C1 and C2 for 0.75 N.

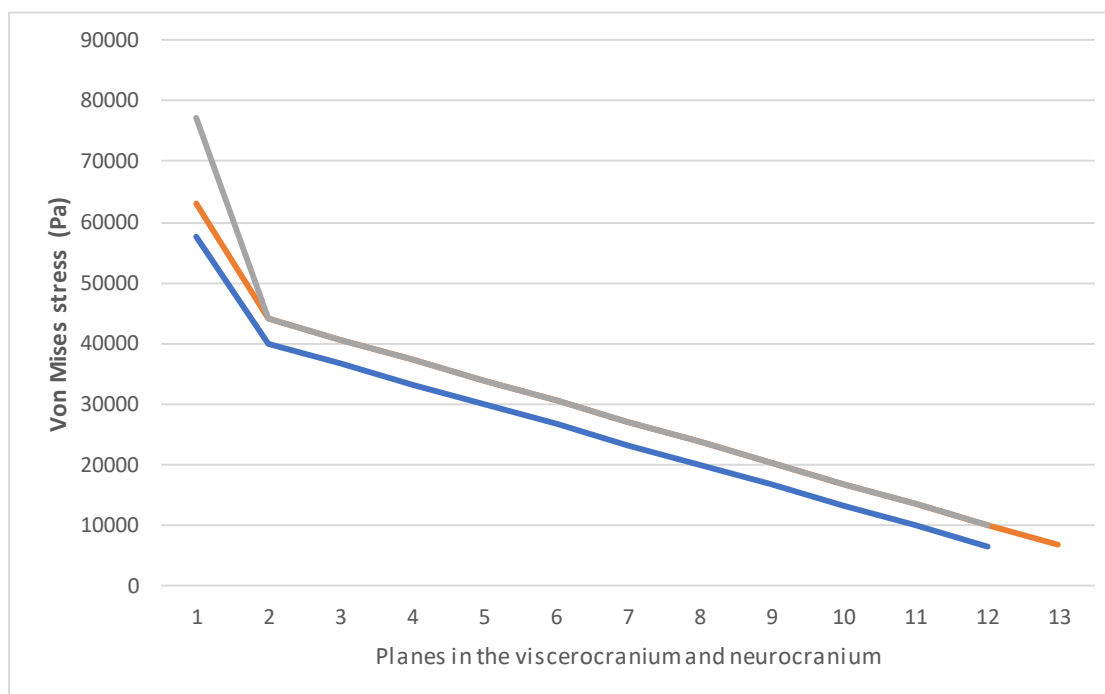


Fig. (3). Comparison of the resulting stress values for each applied force.

The modeling of the infant skull is especially challenging due to its rapid developmental changes and the limited availability of data on infant crania, largely due to restricted access to infant samples [39-41]. The mechanical forces necessary for tissue modeling differ considerably based on factors such as age, bone characteristics, and the particular anatomical area being studied. This highlights the importance of tailored strategies in treatments [42]. Additionally, our understanding of the physical and mechanical forces that shape and alter the size of an infant's skull as it grows after birth remains limited [28]. To address these challenges and overcome data limitations, we chose to use linear elastic models. Linear elastic models are widely used in infant head impact studies because they are simple, require fewer measurements, and are computationally efficient [35, 37, 43]. However, these models cannot fully capture material behavior at high strains or varying conditions, as they assume a linear relationship between stress and strain with no permanent deformation, requiring only two constants for isotropic materials and more for anisotropic materials - five for a transversely isotropic model and nine for an orthotropic model [28]. Research has shown that the elastic modulus and ultimate tensile stress of infant cranial bones and sutures increase with age [31]. In addition, it has been noted that the sutures of infants deform much more than the skull bone before failure suggests brain injury can happen by itself apart from skull fractures [44]. With age-dependent bone properties in mind when generating future infant head models [45].

Similar to previous studies [46], skeletal displacements were analyzed without teeth and periodontal ligament simulation due to the inherent accuracy risk modeling the teeth

and periodontal ligament with CT scans. We modeled only the bony components of the craniofacial skeleton (limited to compact and cancellous bone, excluding teeth and periodontal ligament). Thus, this method provides a more precise evaluation of bone dynamics, specifically regarding cleft lip and palate during Nasoalveolar Molding treatment.

With respect to our results, we hypothesized that deformation is likely to occur based on the level of stress, which could be quantified through pressure developed during point contact. Thus, we established that significant deformation due to stress in positional plagiocephaly likely occurs above a threshold of stress of 30,000 Pa. This value aligned with the results where long-lasting stress over 30,000 Pa gave significant deformation on the viscerocranium and neurocranium [47, 48]. Our findings show that maximum stress values of 77,053 at 0.75 N exceed this distortion threshold, peak potential distortion in the viscerocranium, while lower force (0.65 N and 0.70 N) stay below the threshold, proposing no significant distortion. These findings underscore the importance of observing the stress degree when designing remedy interventions that use mechanical force on the infants' skulls. The threshold we identify may usher clinicians in optimizing NAM therapy to achieve the desired facial shape while avoiding potential long-term distortion.

4.1. Study Limitations and Considerations

The study employed a simplified model of the newborn skull, assuming isotropic and linearly elastic properties, which fails to capture the complex nonlinear behavior of real bone. Age-specific assumptions were primarily based on limited data for a 17-day-old neonate, potentially redu-

cing accuracy when applied to a broader age range. Additionally, the analysis was static and did not account for dynamic forces, infant movements, or variations in pressure distribution during NAM therapy. Furthermore, the reliance on a single patient sample limited the generalizability of the findings to all cases of cleft lip and palate. These limitations highlight the need for more comprehensive models and larger, diverse datasets in future research.

4.2. Future Perspectives

For a better representation of the biomechanics of the baby skull, future studies can concentrate on nonlinear bone properties and use dynamic stimulation to replicate the actual force. As well as individualized 3D models could also enhance treatment precision based on individual anatomical traits.

CONCLUSION

In conclusion, the Finite Element Analysis (FEA) of the neonatal skull with unilateral cleft lip and palate uncovers a significant impact on stress distribution and viscerocranium distortion. Lower applied forces (0.65 N and 0.70 N) did not exceed the distortion threshold of 30,000 Pa, while higher applied force of 0.75 N exceeds the threshold for distortion.

AUTHORS' CONTRIBUTIONS

It is hereby acknowledged that all authors have accepted responsibility for the manuscript's content and consented to its submission. They have meticulously reviewed all results and unanimously approved the final version of the manuscript.

LIST OF ABBREVIATIONS

NAM	=	Nasoalveolar Molding
FEA	=	Finite element analysis
CLP	=	Cleft Lip and Palate
OFC	=	Orofacial Clefts
GV	=	Gray Values

ETHICS APPROVAL AND CONSENT TO PARTICIPATE

The study was approved by the University of Duhok, College of Dentistry -Iraq, under this number (08012025-1-35).

HUMAN AND ANIMAL RIGHTS

All procedures performed in studies involving human participants were in accordance with the ethical standards of institutional and/or research committees and with the 1975 Declaration of Helsinki, as revised in 2013.

CONSENT FOR PUBLICATION

Informed consent was obtained from the guardians.

AVAILABILITY OF DATA AND MATERIALS

The data and supportive information are available within the article.

FUNDING

None.

CONFLICT OF INTEREST

The authors declare no conflict of interest, financial or otherwise.

ACKNOWLEDGEMENTS

Declared none.

REFERENCES

- [1] Salari N, Darvishi N, Heydari M, Bokae S, Darvishi F, Mohammadi M. Global prevalence of cleft palate, cleft lip and cleft palate and lip: A comprehensive systematic review and meta-analysis. *J Stomatol Oral Maxillofac Surg* 2022; 123(2): 110-20. <http://dx.doi.org/10.1016/j.jormas.2021.05.008> PMID: 34033944
- [2] Nasreddine G, El Hajj J. Orofacial clefts embryology, classification, epidemiology, and genetics. *Mutat Res Rev Mutat Res* 2021; 787: 108373. <http://dx.doi.org/10.1016/j.mrrev.2021.108373>
- [3] Jaber HK, Wadood SA. Profile of cleft lip and cleft palate in Basrah province south of Iraq between 2013-2015. *Systemat Rev Pharmacol* 2021; 12(1): 1180-4.
- [4] Leslie EJ, Marazita ML, Eds. Genetics of cleft lip and cleft palate. *Am J Med Genet Part C Semin Med Genet* 2013; 163C(4): 246-58. <http://dx.doi.org/10.1002/ajmg.c.31381>
- [5] Agha B, Helal NMS, Al-Khafaji TJ, Farie GA, Basri O, Fleming PS. Knowledge assessment on cleft lip and palate among recently graduated dentists: A cross-sectional study. *BMC Oral Health* 2023; 23(1): 689. <http://dx.doi.org/10.1186/s12903-023-03388-y> PMID: 37749556
- [6] Geneser MK, Allareddy V. Cleft lip and palate. In: Nowak AJ, Christensen JR, Mabry TR, Townsend JA, Wells MH, Eds. *Pediatric Dentistry (Sixth Edition)*. Amsterdam, Netherlands: Elsevier 2019; pp. 77-87.e2. <http://dx.doi.org/10.1016/B978-0-323-60826-8.00005-5>
- [7] Lee CW, Hwang SM, Lee YS, Kim M-A, Seo KJO. Prevalence of orofacial clefts in Korean live births. *Obstet Gynecol Sci* 2015; 58(3): 196-202. <http://dx.doi.org/10.5468/ogs.2015.58.3.196> PMID: 26023668
- [8] Alswairki HJR, El-Sayed FAA, Fouda MY, Fahim FH, Haque S, Alam MK. *MKJPBeOeCI*. Incidence of Egyptian live births of cleft lip and/or palate in Cairo, Luxor, Aswan and New Valley Governorates: A survey study in 237,783 children. *Pesqui Bras Odontopediatria Clin Integr* 2019; 19(1): 1-9. <http://dx.doi.org/10.4034/PBOCI.2019.191.100>
- [9] Sabbagh HJ, Mossey PA, Innes NPT. Prevalence of orofacial clefts in Saudi Arabia and neighboring countries: A systematic review. *Saudi Dent J* 2012; 24(1): 3-10. <http://dx.doi.org/10.1016/j.sdentj.2011.11.001> PMID: 23960521
- [10] O'Rourke PJP. Advances in cleft lip and palate surgery. *Medicina* 2023; 59(11): 1932.1 Nov. 2023 <http://dx.doi.org/10.3390/medicina59111932>
- [11] Prado F, Rossi A, Freire A, Ferreira Caria P. The application of finite element analysis in the skull biomechanics and dentistry. *Indian J Dent Res* 2014; 25(3): 390-7. <http://dx.doi.org/10.4103/0970-9290.138350> PMID: 25099001
- [12] Ritschl LM, Heinrich V, Grill FD, et al. Stress distribution patterns within viscerocranium and neurocranium during nasoalveolar molding: A finite element analysis. *Plast Reconstr Surg Glob Open* 2018; 6(7): 1832. <http://dx.doi.org/10.1097/GOX.0000000000001832> PMID: 30175012
- [13] Kudagi VS, Shivakumar S, Talwade P. Applications of finite element analysis in dentistry: A review. *J Int Oral Health* 2021; 13(5): 415-22. http://dx.doi.org/10.4103/JIOH.JIOH_11_21

- [14] Syed AUY, Rokaya D, Shahrabaf S, Martin N. Three-dimensional finite element analysis of stress distribution in a tooth restored with full coverage machined polymer crown. *Appl Sci* 2021; 11(3): 1220.
<http://dx.doi.org/10.3390/app11031220>
- [15] Ingawale SM, Goswami T. Design and finite element analysis of patient-specific total temporomandibular joint implants. *Materials* 2022; 15(12): 4342.
<http://dx.doi.org/10.3390/ma15124342> PMID: 35744401
- [16] Qiu P, Cao R, Li Z, Fan Z. A comprehensive biomechanical evaluation of length and diameter of dental implants using finite element analyses: A systematic review. *Heliyon* 2024; 10(5): 26876.
<http://dx.doi.org/10.1016/j.heliyon.2024.e26876> PMID: 38434362
- [17] Popescu AI, Di Francesco P, Bechir A, et al. Finite element analysis (FEA) of the stress behavior of some dental materials. *J Med Life* 2025; 18(1): 29-37.
<http://dx.doi.org/10.25122/jml-2025-0005>
- [18] Shetty P, Hegde A, Rai K. Finite element method--an effective research tool for dentistry. *J Clin Pediatr Dent* 2010; 34(3): 281-5.
<http://dx.doi.org/10.17796/jcpd.34.3.yu44334815546435> PMID: 20578669
- [19] Gazzani F, Pavoni C, Giacchetti A, Cozza P, Lione R. Facemask performance during maxillary protrusion: A finite element analysis (FEA) evaluation of load and stress distribution on Delaire facemask. *Prog Orthod* 2018; 19(1): 21.
<http://dx.doi.org/10.1186/s40510-018-0217-1> PMID: 29984393
- [20] Marcin M, Katarzyna C. Stress and displacement patterns during orthodontic intervention in the maxilla of patients with cleft palate analyzed by finite element analysis: A systematic review. *BMC Oral Health* 2023; 23(1): 93.
<http://dx.doi.org/10.1186/s12903-023-02714-8> PMID: 36782289
- [21] Sasaki A, Takeshita S, Publico AS, et al. Finite element growth analysis for the craniofacial skeleton in patients with cleft lip and palate. *Med Eng Phys* 2004; 26(2): 109-18.
<http://dx.doi.org/10.1016/j.medengphys.2003.10.005> PMID: 15036178
- [22] Li Q, Ren S, Ge C, et al. Effect of jaw opening on the stress pattern in a normal human articular disc: Finite element analysis based on MRI images. *Head Face Med* 2014; 10(1): 24.
<http://dx.doi.org/10.1186/1746-160X-10-24> PMID: 24943463
- [23] Tabassum J. Biomechanical Effects of Maxillary Expansion on a Patient with Bilateral Cleft Lip and Palate--A Finite Element Study. India: Rajiv Gandhi University of Health Sciences 2019.
- [24] Gibson E, Pfeiffauf KD, Skolnick GB, et al. Presurgical orthopedic intervention prior to cleft lip and palate repair: Nasoalveolar molding versus passive molding appliance therapy. *J Craniofac Surg* 2021; 32(2): 486-91.
<http://dx.doi.org/10.1097/SCS.00000000000006929> PMID: 33704966
- [25] Lautner N, Raith S, Ooms M, Peters F, Hölzle F, Modabber A. Three-dimensional evaluation of the effect of nasoalveolar molding on the volume of the alveolar gap in unilateral clefts. *J Craniofac Surg* 2020; 48(2): 141-7.
<http://dx.doi.org/10.1016/j.jcms.2019.12.012> PMID: 31917062
- [26] McPherson GK, Kriewall TJ. The elastic modulus of fetal cranial bone: A first step towards an understanding of the biomechanics of fetal head molding. *J Biomech* 1980; 13(1): 9-16.
[http://dx.doi.org/10.1016/0021-9290\(80\)90003-2](http://dx.doi.org/10.1016/0021-9290(80)90003-2) PMID: 7354097
- [27] Bayen AM, Siau W. An introduction to MATLAB® programming and numerical methods (Interpolation). United States: Academic press 2015; pp. 211-23.
- [28] Brooks T, Choi JE, Garnich M, et al. Finite element models and material data for analysis of infant head impacts. *Heliyon* 2018; 4(12): 01010.
<http://dx.doi.org/10.1016/j.heliyon.2018.e01010> PMID: 30582038
- [29] Tunheim EG, Skalleveold HE, Rokaya D. Role of hormones in bone remodeling in the craniofacial complex: A review. *J Oral Biol Craniofac Res* 2023; 13(2): 210-7.
<http://dx.doi.org/10.1016/j.jobcr.2023.01.009> PMID: 36718389
- [30] Tilotta F, Gosset M, Herrou J, Briot K, Roux C. Association between osteoporosis and periodontitis. *Joint Bone Spine* 2025; 92(4): 105883.
<http://dx.doi.org/10.1016/j.jbspin.2025.105883> PMID: 40090617
- [31] Margulies SS, Thibault KL. Infant skull and suture properties: Measurements and implications for mechanisms of pediatric brain injury. *J Biomech Eng* 2000; 122(4): 364-71.
<http://dx.doi.org/10.1115/1.1287160> PMID: 11036559
- [32] Coats B, Margulies SS, Ji S. Parametric study of head impact in the infant. *Stapp Car Crash J* 2007; 51: 1-15.
<http://dx.doi.org/10.4271/2007-22-0001>
- [33] Roth S, Raul JS, Ludes B, Willinger R. Finite element analysis of impact and shaking inflicted to a child. *Int J Legal Med* 2007; 121(3): 223-8.
<http://dx.doi.org/10.1007/s00414-006-0129-3> PMID: 17091312
- [34] Roth S, Raul JS, Willinger R. Biofidelic child head FE model to simulate real world trauma. *Comput Methods Programs Biomed* 2008; 90(3): 262-74.
<http://dx.doi.org/10.1016/j.cmpb.2008.01.007> PMID: 18342981
- [35] Roth S, Raul JS, Willinger R. Finite element modelling of paediatric head impact: Global validation against experimental data. *Comput Methods Programs Biomed* 2010; 99(1): 25-33.
<http://dx.doi.org/10.1016/j.cmpb.2009.10.004> PMID: 19923034
- [36] Li Z, Luo X, Zhang J. Development/global validation of a 6-month-old pediatric head finite element model and application in investigation of drop-induced infant head injury. *Comput Methods Programs Biomed* 2013; 112(3): 309-19.
<http://dx.doi.org/10.1016/j.cmpb.2013.05.008> PMID: 24008251
- [37] Li Z, Liu W, Zhang J, Hu J. Prediction of skull fracture risk for children 0-9 months old through validated parametric finite element model and cadaver test reconstruction. *Int J Legal Med* 2015; 129(5): 1055-66.
<http://dx.doi.org/10.1007/s00414-015-1190-6> PMID: 25900622
- [38] Li X, Sandler H, Kleiven S. The importance of nonlinear tissue modelling in finite element simulations of infant head impacts. *Biomech Model Mechanobiol* 2017; 16(3): 823-40.
<http://dx.doi.org/10.1007/s10237-016-0855-5> PMID: 27873038
- [39] Motherway JA, Verschuere P, Van der Perre G, Vander Sloten J, Gilchrist MD. The mechanical properties of cranial bone: The effect of loading rate and cranial sampling position. *J Biomech* 2009; 42(13): 2129-35.
<http://dx.doi.org/10.1016/j.jbiomech.2009.05.030> PMID: 19640538
- [40] Rahmoun J, Auperrin A, Delille R, Naceur H, Drazetic P. Characterization and micromechanical modeling of the human cranial bone elastic properties. *Mech Res Commun* 2014; 60: 7-14.
<http://dx.doi.org/10.1016/j.mechrescom.2014.04.001>
- [41] Liang C. Characterising and predicting normal postnatal craniofacial growth and development in human: UCL. UK: University College London 2024.
- [42] Lerebours C, Buenzli PR, Scheiner S, Pivonka P. A multiscale mechanobiological model of bone remodelling predicts site-specific bone loss in the femur during osteoporosis and mechanical disuse. *Biomech Model Mechanobiol* 2016; 15(1): 43-67.
<http://dx.doi.org/10.1007/s10237-015-0705-x> PMID: 26239380
- [43] Li Z, Han X, Ge H, Ma C. A semi-automatic method of generating subject-specific pediatric head finite element models for impact dynamic responses to head injury. *J Mech Behav Biomed Mater* 2016; 60: 557-67.
<http://dx.doi.org/10.1016/j.jmbbm.2016.03.021> PMID: 27058003
- [44] Coats B, Margulies SS. Material properties of human infant skull and suture at high rates. *J Neurotrauma* 2006; 23(8): 1222-32.
<http://dx.doi.org/10.1089/neu.2006.23.1222> PMID: 16928180
- [45] Davis MT, Loyd AM, Shen HH, et al. The mechanical and morphological properties of 6 year-old cranial bone. *J Biomech* 2012; 45(15): 2493-8.
<http://dx.doi.org/10.1016/j.jbiomech.2012.07.001> PMID: 22939291
- [46] Gautam P, Valiathan A, Adhikari R. Maxillary protrusion with and without maxillary expansion: A finite element analysis of sutural

- stresses. Am J Orthod Dentofacial Orthop 2009; 136(3): 361-6.
<http://dx.doi.org/10.1016/j.ajodo.2008.02.021> PMID: 19732670
- [47] Bauer FX, Heinrich V, Grill FD, *et al.* Establishment of a finite element model of a neonate's skull to evaluate the stress pattern distribution resulting during nasoalveolar molding therapy of cleft lip and palate patients. J Craniomaxillofac Surg 2018; 46(4): 660-7.
- [48] Steinberg JP, Rawlani R, Humphries LS, Rawlani V, Vicari FA. Effectiveness of conservative therapy and helmet therapy for positional cranial deformation. Plast Reconstr Surg 2015; 135(3): 833-42.
<http://dx.doi.org/10.1097/PRS.0000000000000955> PMID: 25415272